



Effect of Porosity on the Static Response of Rotating and Non-Rotating Timoshenko Porous Beam

Shashi Chichkhede ^a, Deepak Mahapatra ^b, Shubhashish Sanyal ^a, Shubhankar Bhowmick ^{a,*}

^a Department of Mechanical Engineering, National Institute of Technology Raipur and 492011, India.

^b Department of Agriculture Engineering, Indira Gandhi Krishi Vishwavidyalaya, Raipur and 492011, India.

Abstract

This study aims to determine the effect of porosity on the static response of rotating and non-rotating porous beam. Timoshenko beam theory has been used and the governing equation has been solved via B-spline collocation technique. The material distribution is a function of power law along the height of the beam, even and uneven distribution of porosity has been considered. The parameter such as power index, porosity coefficient and rotational speed have been varied. Deflection and stress variation has been plotted for even and uneven distribution of porosity for relative study. The outcome reveals that effect of even distribution of porosity is higher than uneven porosity. The study also shows that rotation of the beam has significant impact on the deflection and stress distribution of the beam and also reveals that porous beams can be used where high strength and low stiffness is required.

Keywords: Rotating beams; non-rotating beams; functionally graded material; porosity; Static analysis.

1. Introduction

Functionally graded material is an advanced class of tailored materials where the composition of the material changes gradually from one material to another. Thus, making it suitable for incorporating dissimilar functions. Porosity occurring during the manufacture process can affect the performance of the functionally graded material. Presence of the porosity can be utilized to optimize the mechanical characteristics such as strength-to-density and stiffness-to-density. Therefore, many researchers are investigating the effect of porosity distribution in functionally graded material. [1] has discussed various approach for the production of multiscale pores in ceramic monolithic components with different properties such as for, diesel particulate filters, protein sorption, for adding catalytic capabilities, electrical conductivity, piezoelectricity, or ferromagnetic properties to component. A review presented by [2] reported fabrication of porous metal with directional pores and has discussed improved mechanical properties in terms of stress concentration around the pores. The various applications of porous materials has discussed how amount of porosity, pore size, there connectivity and distribution can affect the properties of materials [3].

Analysed functionally graded porous beam where it was established that a better buckling resistance and bending response is obtained in the presence of porosity [4]. On account of prevailing properties of porous material such as light weight, researchers are investigating to enhance the strength of porous structure. A review by [5] present as brief discussion about recent development made on various structure such as arch, beam, shell, and plates.

The paper also discusses about different analysis such as linear, non-linear buckling, bending, free vibration and dynamic response was of structures. Five different type of porosity distribution for higher order deformation theory was reported by [6], where it was determined that various porosity distribution has different effect on the deflection

* Corresponding author. E-mail address: sbhowmick.mech@nitrr.ac.in

of the plate. For even distribution of the porosity the deflection was highest while uneven porosity shows lowest deflection. Static and dynamic study of circular functionally graded porous beam by [7] reveals that higher value of deformation and stresses are obtained in porous beam. Functionally graded non-rotating beam graded in two-direction for various boundary condition was studied by [8, 9] for parabolic shear deformation theory. The author has reported effect of 2-D grading and porosity on various boundary condition. A comparative analysis between layered and functionally graded thick beam was done by [10] to study deflection and stresses developed in material. The results reveal that if correct material grading parameter are used then functionally graded material shows superior behaviour than layered materials.

Under different dynamic load conditions, the dynamic response of multi-layered thick FG beam is investigated [10]. Finite element techniques are used to study time response due to type of force, grading parameter, and sequence of material stacking

The effect of both shear deformation as well as thickness stretching by considering parabolic displacement transverse to the thickness has studied [11]. The effect of porosity bending, and vibration response of the beam was analysed for elastic foundation. Using finite element method, the bending behaviour of rotating porous beam resting on the two-parameter elastic foundation has analysed [12]. The static behaviour of porous beam for even and uneven distribution of porosity reported [13]. The outcome of the paper suggests that even distribution of porosity has higher influence of uneven distribution. The stress and deflection of porous beam based on higher deformation theory are investigated [14]. Various factors such as aspect ratio, material grading, porosity coefficient was considered. Free and forced vibration analysis was done for porous beam according to two different deformation theories [15]. A comparative analysis of porous beam was reported for where a simply supported beam subjected to uniform and sinusoidal load and three different porosity distribution was considered [16]. A rotating Timoshenko nanobeam was studied, where the effect of parameters like external voltage, the thermal stress, the angular velocity, etc. on vibrational frequencies were investigated [17]. The author [18] has also studied the influence of thermo-mechanical load on vibrational behaviour for multilayered piezoelectric nanobeam.

Viscoelastic foundation plays a pivotal role in maintaining stability and performance of structural system, the dynamic behaviour of functionally graded beam resting on nonlinear viscoelastic foundation is investigated [19]. The effect of various parameters such as rise in temperature, material grading, elastic coefficient on damping frequency and deflection is studied. The effect of porosity on composite thick functionally graded beam with viscoelastic foundation as boundary conditions is reported [20]. The results conclude that increasing the elastic stiffness and damping coefficient, a significant reduction of amplitude and oscillation period is observed. Uniform porosity has higher effect than the X and \diamond porosity distribution, however, later is more significant than former porosity distribution. Another paper outlines the impact of dynamic point load on thick FG beam supported by viscoelastic foundation for three different porosity distribution model [21]. The results show influence of parameters like porosity coefficient and distribution, and foundation parameter. The effect of harmonic sinusoidal load on porous FG beam with viscoelastic core is studied [22]. The study reports increase in damping effect due to increase in material viscosity which ultimately decrease in amplitude and oscillation of vibration.

However, static analysis of rotating porous beam is scarce and most of the study has been done on vibrational and buckling characteristics. The functionally graded rotating porous beam, reinforced with graphene platelets for different variable such as porosity coefficient, reinforcement distribution, hub radius etc has studied. were analysed [23]. Decrease in natural frequency was obtained with increase in the porosity coefficient. The axially loaded rotating porous beam and analysed the effect of porosity on the vibrational characteristic has analysed [24]. effect of even and uneven porosity on natural frequency of the rotating beam and stated that for power index less than 0.5 the natural frequency increase, however for power index more than 0.5 the natural frequency decreases due to the presence of porosity [25]. Dynamic behaviour of functionally graded microstructure was analysed for rotating beam and has studied significant impact of material grading and porosity along with slenderness ratio [26]. The author in their paper mentions that the value of material grading has substantial effect on the porosity of the material and in turn changes various static and dynamic behaviour [27].

In the present work, the effect of porosity on rotating and non-rotating beam has been studied on a cantilever beam. According to best of author's knowledge bending and stress analysis of porous rotating beam is limited. Unlike, conventional studies that predominantly focus on homogeneous or functionally graded non-porous materials, this research introduces a unique dimension by incorporating porosity as well as rotational speed into the material composition. By investigating the static bending characteristics of such beams, the paper contributes valuable insights into the mechanical response of functionally graded porous materials, shedding light on a relatively unexplored area within the domain of structural mechanics. This novel approach holds the potential to inform the design and optimization of structures that utilize functionally graded porous materials, thereby expanding the scope of materials engineering and structural analysis. The material properties of the beam are a function of power-law and is varied along the height of the beam. Two types of porosity distribution have been considered i.e., even, and uneven

distribution. A comparative study has been done to examine the effect of rotational speed on the deflection and flexural strength of the material.

2. Nomenclature

A	Area
b	width
B	Position vector of control points
h	Height
L,	Length
L/h	Slenderness ratio
E,	Young's modulus [GPa].
ρ	Density [kg/m^3]
G	Shear modulus along the height of beam [GPa].
u, v, w	Displacement variable in x, y, and z direction
u_0 ,	Axial displacement
t	Knot vectors.
n+1	Number of control points
k	Order of the basis function
k_s	Shear correction factor.
$N_{i,k}(t)$	B-spline basis function
F	Auxiliary function
T_0	Ambient Temperature [K]
ΔT	Temperature distribution across height [K]
K	Thermal Conductivity across height [W/m K]
N_{xx}	Normal force
M_{xx}	Bending moment.
N_T	Thermal force
M_T	Bending moment.
N_R	Centrifugal Force
Q	Shear force.
δU_0	Internal Strain Energy
δU_R	Work done due to centrifugal force.
δU_P	Work done due to uniformly distributed load by 'q.'
$\epsilon_{xx}, \gamma_{xz}$	Normal strain and shear strain
σ_{xx}, τ_{xz}	Normal stress and Shear stress
Ω	Rotational speed [rad/sec]
μ	Poisson's ratio
μ	Power index
λ	Thermal expansion coefficient [$^{\circ}\text{K}$]
α	Rotation of mid-plane
θ	

3. Theoretical Formulation:

3.1. Description of model:

Consider a functionally graded (FG) porous Timoshenko beam as shown in Fig 1(a). The length of the beam 'L' is along the x -direction while the cross-section with width 'b' and 'h' in along z-y plane. One end is fixed about which the beam rotates with rotational speed of Ω rad/sec, and the other end is free.

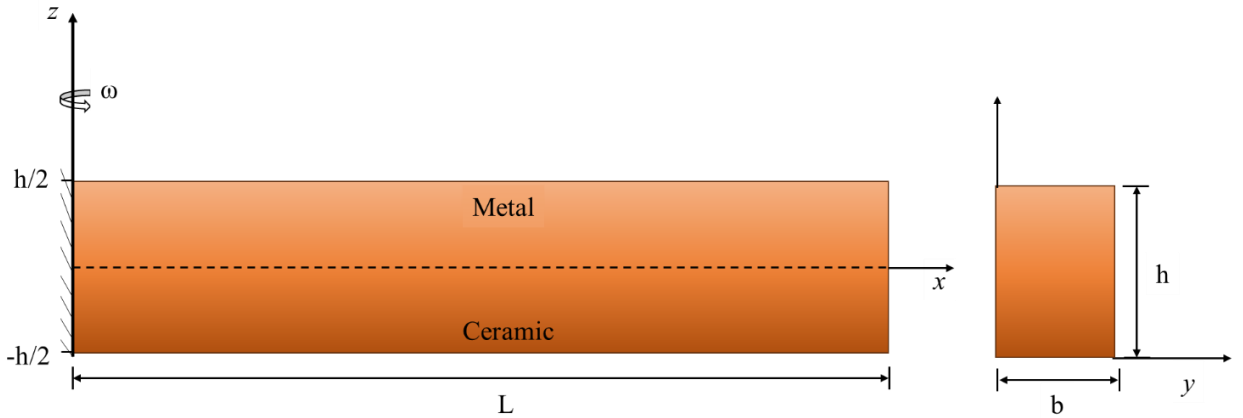


Fig 1: Functionally Graded Cantilever Beam.

3.2. Material properties of functionally graded porous beam:

The functionally graded material is developed by continuously grading metal and ceramic along the height of the beam. The topmost surface is metal-rich ($z = h/2$) and bottommost surface is ceramic-rich ($z = -h/2$). The material distribution along the height of the beam is a function of power law where the volume fraction of ceramic V_c is given by eqn.1 and V_m by eqn.2:

$$V_c = \left(\frac{z}{h} + \frac{1}{2} \right)^\lambda, \tag{2.1}$$

$$V_m = 1 - V_c, \tag{2.2}$$

with $\lambda \geq 0$

Where Volume fraction of ceramic varies in z-direction, λ is power index. Ceramic is denoting as ‘c’ and metal is denoting as ‘m’.

During fabrication process materials are susceptible to manufacturing defects such as porosities [2]. The imperfection due to porosity in the functionally graded material can be distributed two ways i.e., even, and uneven distribution of porosity. Fig 2(a), Fig 2(b). shows even and uneven distribution of porosity across the height of the beam.

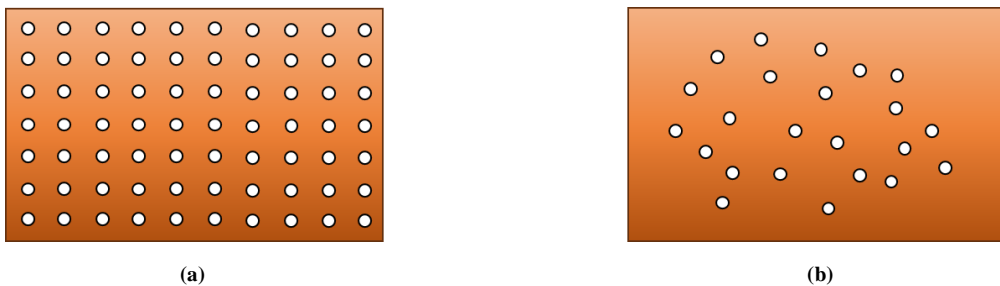


Fig 2: (a) Even Distribution of porosity, (b) Uneven Distribution of porosity across the height of the beam.

The material properties P, such as Young’s modulus E, densities ρ , and expansion coefficient α vary along the height i.e., in z-direction. Based on Voigt’s rule [28], the effective material properties are predicted as:

$$P(z) = (P_c - P_m) \left(\frac{z}{h} + \frac{1}{2} \right)^2 + P_m - \frac{\alpha}{2} (P_c + P_m), \quad (\text{Even Porosity}) \quad (2.3)$$

$$P(z) = (P_c - P_m) \left(\frac{z}{h} + \frac{1}{2} \right)^2 + P_m - \frac{\alpha}{2} (P_c + P_m) \left(1 - \frac{2|z|}{h} \right), \quad (\text{Uneven Porosity}) \quad (2.4)$$

3.3. Governing condition and Boundary Condition:

Timoshenko's beam theory was used to include the effect of shear deformation, assuming that a line across the axis of the beam remains before deformation. (1) Straight (2) Inelastic (3) Rotation is independent to the slope of the beam. The displacement along x, y, z-direction is given in eqn.5:

$$u(x, z) = u_0(x) + z\theta \quad (2.5a)$$

$$v(x, z) = 0 \quad (2.5b)$$

$$w(x, z) = w_0(x) \quad (2.5c)$$

u_0 , w_0 and θ are the axial displacement, transverse displacement, and rotation of the midplane, respectively in eqn. (6) and these represent the strains using von-Karman theory on account of moderately large deflection and small strain. Therefore, strains according to this theory are given as in [29] by eqn. (6):

$$\varepsilon_{xx} = \left(\frac{\partial u_0}{\partial x} + \frac{1}{2} \left(\frac{\partial w_0}{\partial x} \right)^2 \right) + \left(z \frac{\partial \theta}{\partial x} \right), \quad (2.6a)$$

$$\gamma_{xz} = \left(\frac{\partial w_0}{\partial x} + \theta \right) \quad (2.6b)$$

ε_{xx} , and γ_{xz} , are mechanical strain and shear strain respectively. Principle of virtual work is used to derive the governing equation of rotating beam where the sum of the virtual work done by internal (I) and external force (E) is zero i.e.,

$$(\delta U_0)_I - (\delta U_R + \delta U_P)_E = 0 \quad (2.7)$$

Where, δU_0 , δU_R and δU_P are strain energy, work done due to rotation and work done due to uniformly distributed load respectively. In case of non-rotating beam, the work done due to rotation i.e., δU_R will be ignored.

Strain energy of the beam is defined as δU_0 :

$$\begin{aligned} \delta U_0 &= \int_0^L \int_A (\sigma_{xx} \delta \varepsilon_{xx} + \tau_{xz} \delta \gamma_{xz}) dA dx \\ \delta U_0 &= \int_0^L N_{xx} \delta \varepsilon_{xx} + Q_{xz} \delta \gamma_{xz} dx \\ \delta U_0 &= \int_0^L \left(N_{xx} \delta \left(\frac{\partial u_0}{\partial x} + \frac{1}{2} \left(\frac{\partial w_0}{\partial x} \right)^2 + z \left(\frac{\partial \theta}{\partial x} \right) \right) + Q_{xz} \delta \left(\frac{\partial w_0}{\partial x} + \theta \right) \right) dx \end{aligned} \quad (2.8)$$

Here, N_{xx} is the axial force, M_{xx} is bending moment, and Q_{xz} is shear force. This resultant is expressed as eqn. (9):

$$N_{xx} = \int_A \sigma_{xx} dA, \quad M_{xx} = \int_A z \cdot \sigma_{xx} dA, \quad Q_{xz} = \int_A k_s \cdot \tau_{xz} dA \quad (2.9)$$

The external work done due to uniformly distributed load 'q₀' is defined as δU_P :

$$\delta U_P = b \int_0^L q_0(x) \cdot w_0(x) \cdot dx \tag{2.10}$$

The work done due to centrifugal force on the beam is defined as δU_R [12]:

$$\delta U_R = \frac{1}{2} \int_0^L N_R \cdot \frac{\partial w}{\partial x} \cdot \frac{\partial \delta w}{\partial x} \cdot dx \tag{2.11}$$

And

$$N_R = \int \int_{Ax} \rho \Omega^2 (R+x) dA dx$$

$$N_R = \rho A \Omega^2 (R(L-x) + \frac{L^2 - x^2}{2}) \tag{2.12}$$

Equation for the internal and external work done i.e., eqns. (8), (10), and (11) is substituted in eqn. (7) and setting the coefficient of δu , $\delta \theta$, δw to zero, the following Euler–Lagrange equation can be obtained.

$$\delta u: \quad \frac{\partial N_{xx}}{\partial x} = 0 \tag{2.13}$$

$$\delta \theta: \quad \frac{\partial M_{xx}}{\partial x} - Q_{xz} = 0 \tag{2.14}$$

$$\delta w: \quad \frac{\partial^2 M_{xx}}{\partial x^2} - \frac{\partial}{\partial x} \left(N_{xx} \frac{\partial w}{\partial x} \right) + \frac{\partial}{\partial x} \left(N_R \frac{\partial w}{\partial x} \right) + q = 0 \tag{2.15}$$

Under the following boundary conditions at:

$x = 0$	$x = L$
$\delta u = 0$	$N_{xx} = 0$
$\delta \theta = 0$	$M_{xx} = 0$
$\delta w = 0$	$Q_{xz} = 0$

Further, from [30]:

$$w = F - \frac{\hat{E}_2}{G_0} \frac{d^2 F}{dx^2}, \quad \theta = -\frac{dF}{dx} \tag{2.16}$$

where ‘F’ is a new auxiliary function of length dimension. Simplifying eqns. (13), (14), and (15), and thereby converting these into single fourth order equation of single unknown variable as follows.

$$\hat{E}_2 \left(1 - \frac{N_R}{G_0} \right) \left(\frac{d^4 F}{dx^4} \right) - \frac{\hat{E}_2}{G_0} \frac{dN_R}{dx} \frac{d^3 F}{dx^3} + N_R \frac{d^2 F}{dx^2} + \frac{dN_R}{dx} \frac{dF}{dx} = q \tag{2.17}$$

Eqn. (17) describes governing equation for rotating beam, for non-rotation beam, in the same equation the term N_R is taken as zero and following equation is obtained:

$$\hat{E}_2 \left(\frac{d^4 F}{dx^4} \right) = q \quad (2.18)$$

In eqn. (17)-(18), \hat{E}_2 represent:

$$\hat{E}_2 = E_2 - \frac{E_1^2}{E_0}$$

E_0, E_1, E_2 is expressed as:

$$[E_0, E_1, E_2] = \int_A E(z)(1, z, z^2) dA \quad (2.19)$$

The bending moment and shear force can be expressed in terms of auxiliary function F as

$$M_{xx} = \hat{E}_2 \frac{d^2 F}{dx^2}, \quad Q = \hat{E}_2 \frac{d^3 F}{dx^3} \quad (2.20)$$

3.4. Solution Procedure:

To solve the governing equation for functionally graded cantilever beam B-spline collocation method was used. B-spline collocation method provides piecewise continuous solution where the differential equation is satisfied at a finite number of points called collocation points. The parametric coordinate 't' defines the order of the resulting polynomial, also known as the knot vector. It is assumed that the knot vector is of open type given by following expression.

$$T = [t_0, t_1, t_2, \dots, t_{n+k+1}] \quad (2.21)$$

Where, $n+1$ are the number of control points and 'k' is the order of the polynomial spline. Cox-de Boor recursion formula has been used to define the B-spline basis function $N_{i,k}(t)$ and is calculated as

$$N_{i,1}(t) = \begin{cases} 1, & x_i \leq t \leq x_{i+1} \\ 0, & \text{otherwise} \end{cases} \quad (2.22)$$

$$N_{i,k}(t) = \frac{(t - x_i)N_{i,k-1}(t)}{x_{i+k-1} - x_i} + \frac{(x_{i+k} - t)N_{i+1,k-1}(t)}{x_{i+k} - x_{i+1}} \quad (2.23)$$

$(n+1)$ control points, $B_0, B_1, B_2, \dots, B_n$ and basis functions are used to define the B-spline curve.

$$F(t) = \sum_{i=1}^{n+1} B_i N_{i,k}(t) \quad (2.24)$$

Here,

$$t_{min} \leq t \leq t_{max}, 2 \leq k \leq n+1 \quad (2.25)$$

't' is the parametric coordinate used to define the position vector of the control point 'Bi' is given by equation given below. Collocation points or abscissa control points are selected using the Grevillea abscissa approach.

$$x_i = \frac{1}{n} (t_i + t_{i+1} + \dots + t_{i+n-1}) \quad (2.26)$$

In the present study, an in-house MATLAB code is developed indigenously to numerically investigate the problem of rotating FG beams. Higher order B-spline function is chosen to investigate response of the beam in the presence of material and geometric non-linearity.

4. Results and Discussion

In this segment, functionally graded (FG) porous beam is examined to analyse the effect of porosity on rotating and non-rotating beams. Two different types of porosity distribution have been considered i.e., even, and uneven porosity. The material for FG beam considered are Aluminium (Al) and Alumina (Al₂O₃) and the properties of the material are as follows [13]:

- Aluminium, (Metal): $E_m = 70 \text{ GPa}; \quad \rho_m = 2707 \text{ Kg/m}^3; \quad \nu = 0.3$
- Alumina, (Ceramic) $E_c = 380 \text{ GPa}; \quad \rho_c = 3960 \text{ Kg/m}^3; \quad \nu = 0.3$

In the present study, the top surface is metal rich and bottom surface is ceramic rich.

4.1. Validation:

In order to validate the proposed model a simply supported FG beam is considered with $L/h = 5, \lambda = 2$. The FG porous beam is subjected to uniformly distributed load of $q = 1 \times 10^6 \text{ N}$ on the top surface of the beam. The non-dimensional central deflection at the $w(L/2)$ obtained in the present work is compared with other beam theories [9, 11] at porosity $\alpha = 0, 0.1, 0.2$ shown in table.1. The non-dimensional parameter for comparison of deflection is given as:

$$\bar{w}, ref(L/2) = w(L/2).100 \frac{E_m \cdot I}{q \cdot L^4}, \quad \bar{\sigma}_{xx} = \frac{\sigma_{xx} \cdot b \cdot h}{q \cdot l}(L/2),$$

$$\bar{\tau}_{xx} = \frac{\tau_{xx} \cdot b \cdot h}{q \cdot l}(L/2)$$

In second case, a cantilever beam with $L/h = 5$ and $\lambda = 0, 1$ have be used to check the validity of model for rotating beam. The beam is rotated at rotational speed of $\Omega = 100 \text{ rad/sec}$, and deflection of the beam is compared to that of the results obtained from FEA software ANSYS. The beam is modelled using element PLANE183. The results are listed in the table.2 for rotating beam:

Table1: Non-dimensional deflection at the centre of the beam at different value of porosity and with $\lambda = 2, L/h = 5$.

Porosity	Present work	[11]	Error%	[9]	Error%
0	5.196649483	5.2	0.064%	5.35	2.866%
0.1	5.827938436	5.82	-0.136%	6.22	6.303%
0.2	6.652521785	6.63	-0.340%	7.38	9.857%

Table2: Dimensional transverse deflection of cantilever beam at free end for $\lambda = 0, 1; L/h = 5$ and $\Omega = 100 \text{ rad/sec}$.

Power Index, λ	Present work	FEA software	Error %
0	-2.42453E-06	-2.4165E-06	-0.33%
1	-8.94655E-07	-9.0461E-07	1.10%

The present works shows good agreement with the available literature and FEA software. And presents accuracy and reliability of the current method.

4.2. Parametric study

- Non-Rotating Beam:

Cantilever beam subjected to uniformly distributed load of $q = 10^6 \text{ N/m}^2$ and length to thickness ratio of $L/h = 10$ is considered. Aluminium and alumina are used for functionally graded material whose properties are mentioned above. Deflection at the free end of the beam along with increase in the porosity is plotted in Fig.3 at different value of power index for even and uneven porosity. Magnitude of deflection increases with increase in the value of porosity. A substantial increment of deflection at higher value of porosity can be seen. At $\lambda = 0.5$ and at $\alpha = 0.35, 0.4$ deflection of the beam unusually exceeds the metal. For pure metal a linear increase is noted. Further, with increase in the value of porosity the value of deflection increases. This is possibly due to decrease in the stiffness of the beam with increase of porosity. The influence of porosity reduces as the power index increases where for pure metal deflection is highest and pure ceramic deflection is lowest due to increase in the stiffness material. Uneven porosity shows lower magnitude of deflection as compared to the even porosity and the effect of porosity on metal is way higher than at different power

index due to least stiffness.

Normalized axial stress along the height of the beam at fixed end is plotted in Fig.4 for various value of porosity i.e., $\alpha = 0, 0.2, 0.4$ and at power index $\lambda = 1$. Results shows that with increase in porosity the axial compressive stress at bottom fibre also increases, whereas in the top fibre axial stress decreases and even shows compressive stress at $\alpha = 0.4$. Fig.4(a) shows axial stress for even porosity, where the stress increases linearly along certain height of the beam and the slop of the stress decreases with porosity. The axial stress then forms a curve, wherein the curvature of this curve increases with increase in the porosity and shows tensile behaviour. Finally, the axial stress towards the top fibre decreases, however, a transition in the nature of stress is observed with increases in porosity i.e., at $\alpha = 0.2$, the nature of the stress is tensile and at $\alpha = 0.4$, the stress shows compressive behaviour. Functional grading causes the neutral axis to shift below the centroidal axis due to which compressive stress can be seen between $z/h = -0.5$ to -0.1 , and tensile stress above $z/h = -0.20$. For uneven porosity the variation of the axial stress along the height of the beam as shown in Fig.4(b) increases with increase in porosity. Unlike even porosity, uneven porosity shows parallel increase in the axial stress with increase of porosity and does not intersect each other.

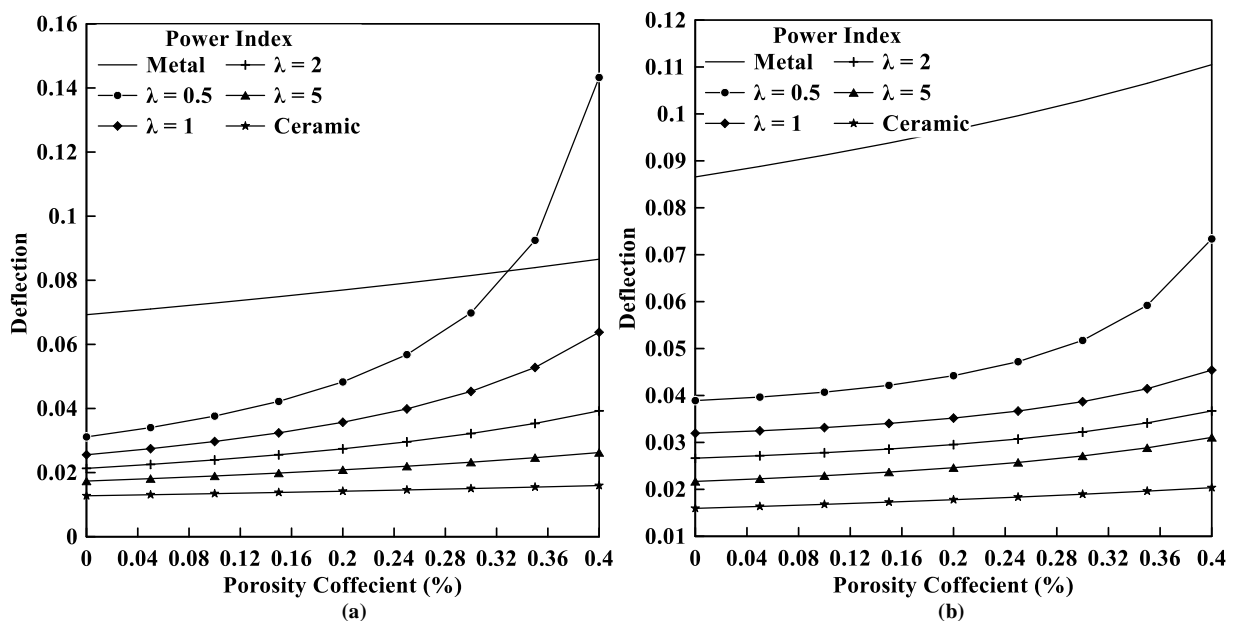


Fig 3: No-dimensional deflection of beam with respect to porosity of (a) Even (b) uneven distribution for various value of power index.

At fixed end the effect of porosity on shear stress along the height of the beam is plotted in Fig.5 for even and uneven distribution of porosity i.e., $\alpha = 0, 0.2, 0.4$ at power index of $\lambda = 1$. For both even and uneven distribution of porosity the value of shear stress at bottom fibre is zero however at the top fibre the shear stress is non-zero and increases with increase in porosity. The value of maximum shear stress increases with increase of porosity, in addition to this the position of maximum shear stress can be seen shifting below the centroidal axis for even distribution of porosity and above the centroidal axis for uneven distribution of porosity.

- **Rotating Beam:**

In this section, the paper discusses the influence of rotation on the porosity of a rotating beam. Inducing porosity reduces the stiffness of the beam however effect of centrifugal force due rotation needed to be discussed. Deflection of beam rotating at $\Omega = 200$ rad/sec with respect to the even and uneven porosity at different value of power index is plotted in Fig.6. Results shows that deflection increases with increase in porosity however deflection decreases with increase in power index for both even and uneven distribution of porosity. On comparing the results of Fig.3 and Fig.6 it is ascertained that deflection in rotating beam is higher than non-rotation beam for both even and uneven porosity. The increase in deflection with porosity for metal is very subtle. Whereas for graded material, towards higher value of porosity a considerable value of deflection can be seen specifically at $\lambda = 0.5$. This suggests that rotation assist in

reducing the stiffness of beam. The Effect of rotating speed on the deflection can be observed in Fig.7 plotted at porosity, $\alpha = 0, 0.2, 0.4$. With increasing value of rotational speed, deflection goes on increasing. The effect of rotation speed is higher at higher value of porosity specifically at $\alpha = 0.4$, in case on non-porous beam i.e., $\alpha = 0$ the variation of deflection due to rotating speed is lower because of higher stiffness as compared to porous beam. For uneven distribution of porosity Fig.7(b) although there is increment in the deflection with rotational speed as well as porosity, but deflection is lower as against the even distribution of porosity.

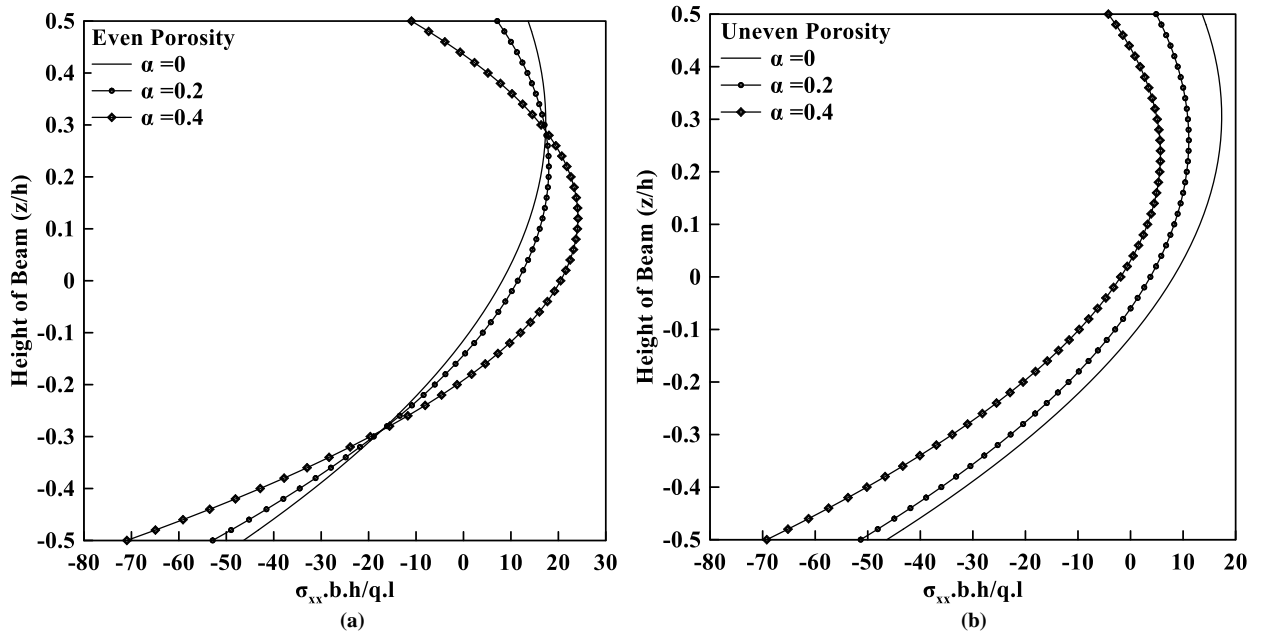


Fig 4: Axial stress along the height of the beam at different value of porosity for (a) Even (b) uneven distribution at power index $\lambda=1$.

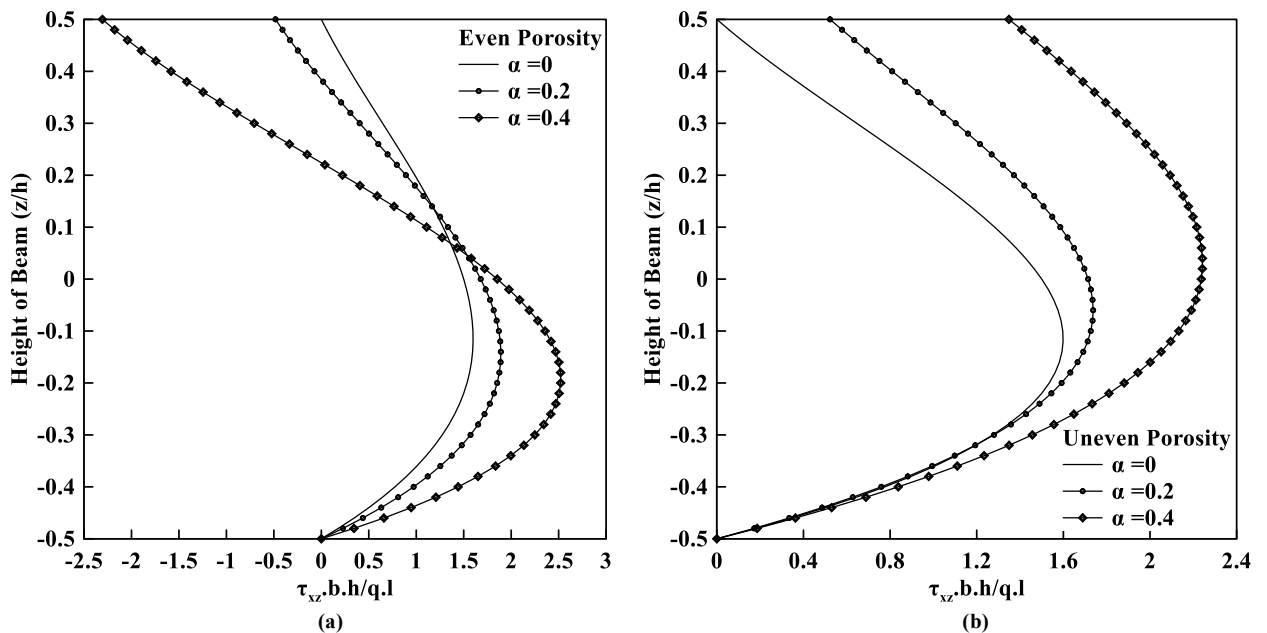


Fig 5: Shear stress along the height of the beam at different value of porosity for (a) Even (b) uneven distribution at power index $\lambda=1$.

Influence of rotation on axial stress distribution is plotted in Fig.8 in the transvers direction at $\alpha = 0, 0.2, 0.4$. The beam is rotated at the speed of $\Omega = 400$ rad/sec at constant value of $\lambda = 1$. The graph plotted shows that rotating beam induce higher stress as compared to the non-rotating beams. The stress at bottom fibre increases with increase of porosity while at top fibre decreases for both even and uneven rotating beam. For even porous beam, Fig.8(a) shows fluctuating behaviour where at $\alpha = 0.4$ due to rotation. The reason for such a behaviour could be that at higher porosity

density of the beam reduces and due to rotation, a net moment is created that lifts the beam in upward direction. Again, the value of axial stress increases linearly from bottom surface along transverse direction and forms a curve towards the top surface and then again decreases at the top surface. For uneven-porous rotating beam shown in Fig. 8(b) at $\alpha = 0.4$ shows higher curvature towards the top fibre of the beam and axial stress develop at bottom surface is way higher than at lower value of α .

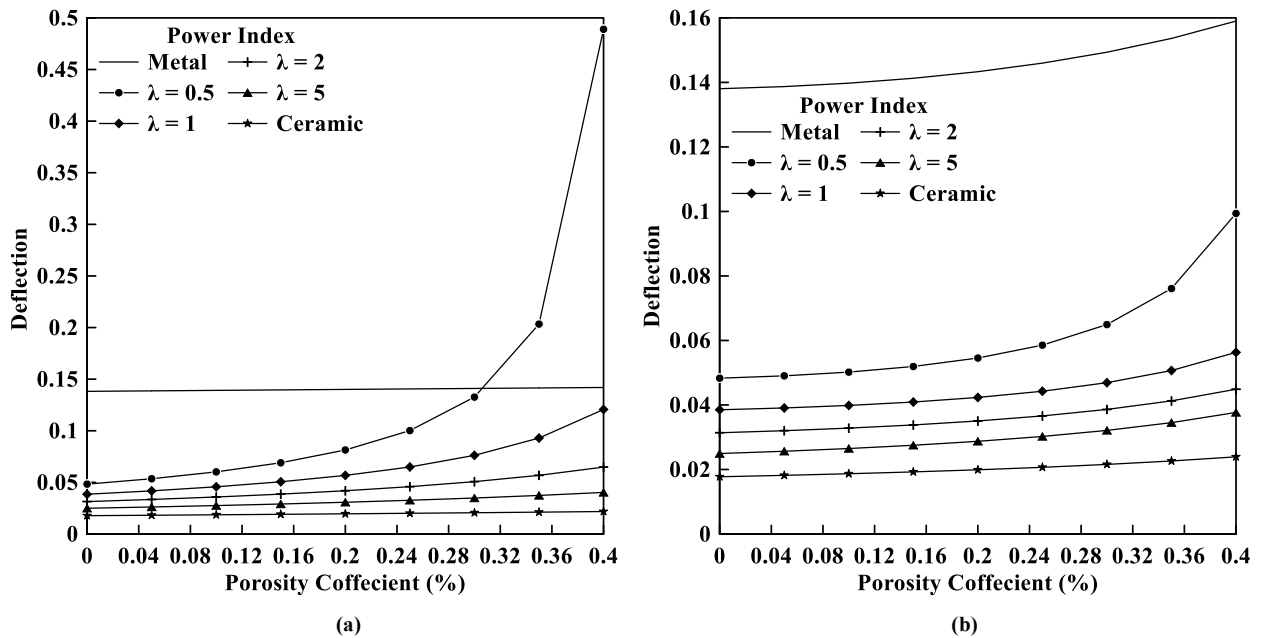


Fig 6: Deflection of beam rotating at $\Omega = 200$ rad/sec with respect to the porosity of (a) Even (b) uneven distribution for various value of power index.

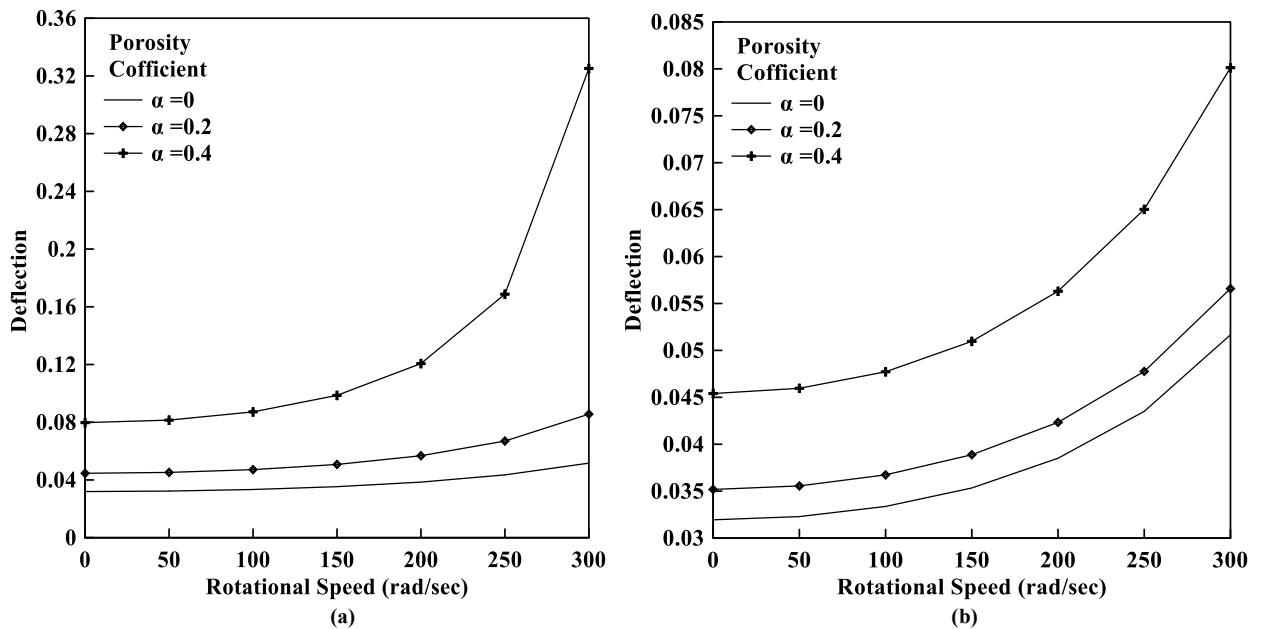


Fig 7: Deflection of beam with respect to the rotating speed for various value of (a) Even (b) uneven distribution porosity at power index $\lambda = 1$.

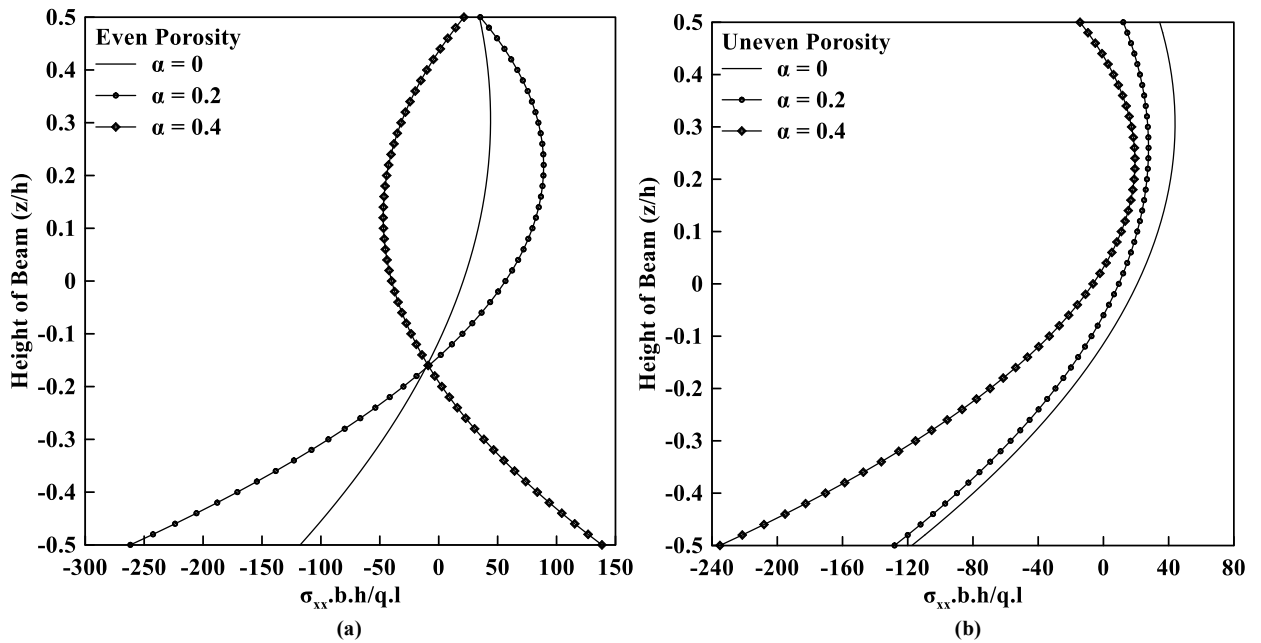


Fig 8: Axial stress along the height of the beam rotating at $\Omega = 400$ rad/sec different value of porosity for (a) Even (b) uneven distribution at power index $\lambda=1$.

Shear stress distribution for even and uneven distribution of porosity of $\alpha = 0, 0.2, 0.4$ is at $\lambda = 1$ and $\Omega = 400$ rad/sec shown in the Fig.9. Again, the shear stress obtained for rotating porous beam is higher than non-rotating porous beam. The value of shear stress is zero at the bottom fibre for even and uneven distribution of porosity while non-zero at top fibre. In Fig.9(a) for even distribution of porosity, with increase in porosity the shear stress increases but is compressive in nature at the top surface while, for uneven distribution of porosity, shear stress shows tensile nature at top surface. Also, the position of maximum stress moves towards bottom surface for even porosity whereas for uneven distribution of porosity the position of maximum stress moves towards top surface.

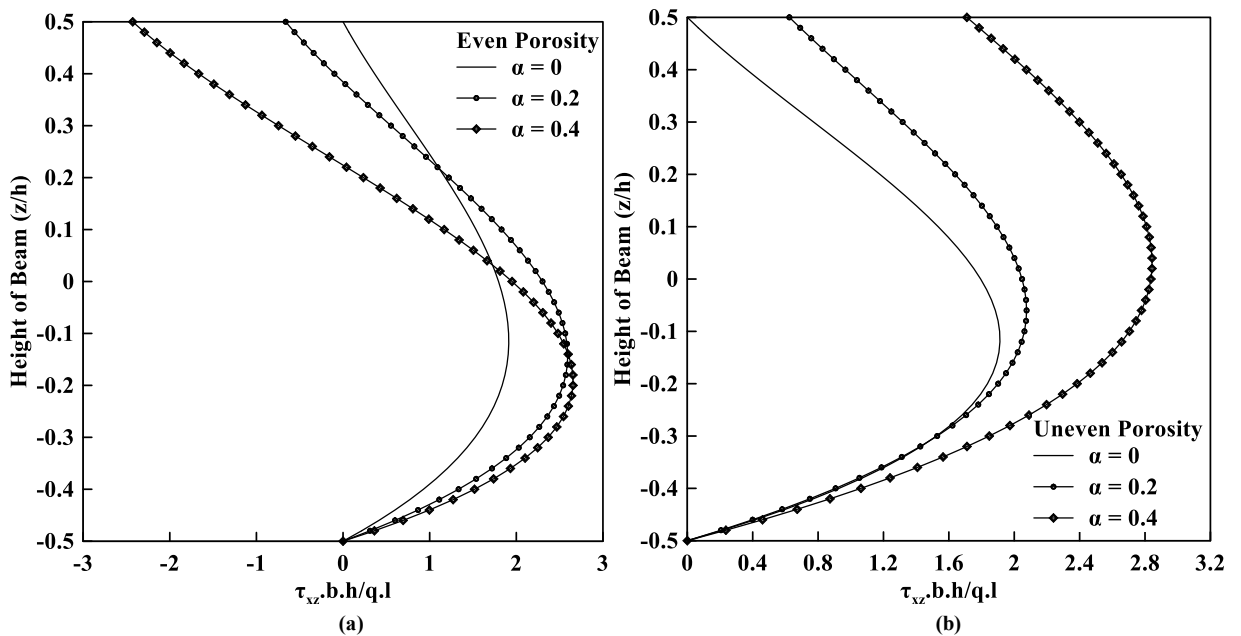


Fig 9: Shear stress along the height of the beam rotating at $\Omega = 400$ rad/sec different value of porosity for (a) Even (b) uneven distribution at power index $\lambda=1$.

5. Conclusion:

The aim of this work is to investigate the effect of porosity on beams under rotating and non-rotating conditions. Timoshenko beam theory was applied with the consideration of even and uneven distribution of porosity was considered. To solve this problem B-spline collocation method was used and a MATLAB code was developed for the same. The results indicate that effect of even distribution of porosity is higher than uneven distribution. Porosity reduces the stiffness of the material therefore an increase in the value of deflection was obtain with increase in the porosity. However, an increase in the values of stresses was obtained with increment in the porosity. Similarly, in case of rotating beam the value of deflection and stresses increases with increase in the porosity. The outcome also shows that with increase in the speed the magnitude of deflection also increases exhibiting consequences of rotation. As compared to non-rotating beam rotating beam displays higher value of different parameter.

Acknowledgements

The authors gratefully acknowledge National institute of technology, Raipur for their support and providing platform for this research.

References

- [1] P. Colombo, C. Vakifahmetoglu, S. Costacurta, Fabrication of ceramic components with hierarchical porosity, *Journal of Materials Science*, Vol. 45, No. 20, pp. 5425-5455, 2010/10/01, 2010.
- [2] H. Nakajima, Fabrication, properties and application of porous metals with directional pores, *Progress in Materials Science*, Vol. 52, No. 7, pp. 1091-1173, 2007/09/01/, 2007.
- [3] P. Colombo, Materials science. In praise of pores, *Science*, Vol. 322, No. 5900, pp. 381-3, Oct 17, 2008. eng
- [4] D. Chen, J. Yang, S. Kitipornchai, Elastic buckling and static bending of shear deformable functionally graded porous beam, *Composite Structures*, Vol. 133, pp. 54-61, 2015/12/01/, 2015.
- [5] H. Wu, J. Yang, S. Kitipornchai, Mechanical Analysis of Functionally Graded Porous Structures: A Review, *International Journal of Structural Stability and Dynamics*, Vol. 20, No. 13, pp. 2041015, 2020.
- [6] M. Dhuria, N. Grover, K. Goyal, Influence of porosity distribution on static and buckling responses of porous functionally graded plates, *Structures*, Vol. 34, pp. 1458-1474, 2021/12/01/, 2021.
- [7] A. S. Sayyad, P. V. Avhad, L. Hadji, On the static deformation and frequency analysis of functionally graded porous circular beams, *Forces in Mechanics*, Vol. 7, pp. 100093, 2022/05/01/, 2022.
- [8] M. Turan, G. Adiyaman, A New Higher-Order Finite Element for Static Analysis of Two-Directional Functionally Graded Porous Beams, *Arabian Journal for Science and Engineering*, Vol. 48, 03/24, 2023.
- [9] O. Kirlangıç, Ş. D. Akbaş, Comparison study between layered and functionally graded composite beams for static deflection and stress analyses, *Journal of Computational Applied Mechanics*, Vol. 51, No. 2, pp. 294-301, 2020.
- [10] M. A. Eltahir, Ş. D. Akbaş, Transient response of 2D functionally graded beam structure, *Structural Engineering and Mechanics, An Int'l Journal*, Vol. 75, No. 3, pp. 357-367, 2020.
- [11] A. A. Hassen, A. Tounsi, F. Bernard, Effect of thickness stretching and porosity on mechanical response of a functionally graded beams resting on elastic foundations, *International Journal of Mechanics and Materials in Design*, Vol. 13, pp. 71-84, 03/01, 2017.
- [12] N. Dang, Finite Element Modeling for Static Bending Behaviors of Rotating FGM Porous Beams with Geometrical Imperfections Resting on Elastic Foundation and Subjected to Axial Compression, *Advances in Materials Science and Engineering*, Vol. 2021, pp. 1-15, 12/10, 2021.
- [13] S. Zghal, D. Ataoui, D. Fakhreddine, Static bending analysis of beams made of functionally graded porous materials, *Mechanics Based Design of Structures and Machines*, Vol. 50, pp. 1-18, 04/08, 2020.
- [14] S. Merdaci, H. Belghoul, High-order shear theory for static analysis of functionally graded plates with porosities, *Comptes Rendus Mécanique*, Vol. 347, No. 3, pp. 207-217, 2019/03/01/, 2019.
- [15] D. Wu, A. Liu, Y. Huang, Y. Huang, Y. Pi, W. Gao, Dynamic analysis of functionally graded porous structures through finite element analysis, *Engineering Structures*, Vol. 165, pp. 287-301, 2018/06/15/, 2018.
- [16] C. T. Binh, T. H. Quoc, D. T. Huan, H. T. Hien, Vibration characteristics of rotating functionally graded porous beams reinforced by graphene platelets, *Journal of Science and Technology in Civil Engineering (JSTCE)-HUCE*, Vol. 15, No. 4, pp. 29-41, 2021.

- [17] M. Mohammadi, A. Farajpour, A. Moradi, M. Hosseini, Vibration analysis of the rotating multilayer piezoelectric Timoshenko nanobeam, *Engineering Analysis with Boundary Elements*, Vol. 145, pp. 117-131, 2022/12/01/, 2022.
- [18] M. Mohammadi, A. Farajpour, A. Rastgoo, Coriolis effects on the thermo-mechanical vibration analysis of the rotating multilayer piezoelectric nanobeam, *Acta Mechanica*, Vol. 234, No. 2, pp. 751-774, 2023/02/01, 2023.
- [19] M. Alimoradzadeh, S. Akbas, Nonlinear thermal vibration of FGM beams resting on nonlinear viscoelastic foundation, *Steel and Composite Structures*, Vol. 44, No. 4, pp. 557, 2022.
- [20] Ş. Akbaş, A. Bashiri, A. Assie, M. A. Eltaher, Dynamic analysis of thick beams with functionally graded porous layers and viscoelastic support, *Journal of Vibration and Control*, Vol. 27, pp. 107754632094730, 08/03, 2021.
- [21] A. Alnujaie, Ş. Akbaş, M. A. Eltaher, A. Assie, Forced vibration of a functionally graded porous beam resting on viscoelastic foundation, *Geomechanics and Engineering*, Vol. 24, 02/10, 2021.
- [22] A. Assie, Ş. Akbaş, A. Kabeel, A. Alaa, M. A. Eltaher, Dynamic analysis of porous functionally graded layered deep beams with viscoelastic core, *Steel and Composite Structures*, Vol. 43, pp. 79-90, 04/13, 2022.
- [23] N. Giang, Free Vibration Exploration of Rotating FGM Porosity Beams under Axial Load considering the Initial Geometrical Imperfection, *Mathematical Problems in Engineering*, Vol. 2021, pp. 1-16, 03/18, 2021.
- [24] M. Amoozgar, L. Gelman, Vibration analysis of rotating porous functionally graded material beams using exact formulation, *Journal of Vibration and Control*, Vol. 28, pp. 107754632110278, 06/22, 2021.
- [25] F. Ebrahimi, M. Mokhtari, Transverse vibration analysis of rotating porous beam with functionally graded microstructure using the differential transform method, *Journal of the Brazilian Society of Mechanical Sciences and Engineering*, Vol. 37, 10/01, 2014.
- [26] F. Ebrahimi, M. Hashemi, On vibration behavior of rotating functionally graded double-tapered beam with the effect of porosities, *Proceedings of the Institution of Mechanical Engineers, Part G: Journal of Aerospace Engineering*, Vol. 230, 12/11, 2015.
- [27] F. Ebrahimi, E. Salari, S. Hosseini, Thermomechanical Vibration Behavior of FG Nanobeams Subjected to Linear and Non-Linear Temperature Distributions, *Journal of Thermal Stresses*, Vol. 38, pp. 1362-1388, 12/02, 2015.
- [28] M. Mohammadi, M. Hosseini, M. Shishesaz, A. Hadi, A. Rastgoo, Primary and secondary resonance analysis of porous functionally graded nanobeam resting on a nonlinear foundation subjected to mechanical and electrical loads, *European Journal of Mechanics - A/Solids*, Vol. 77, pp. 103793, 2019/09/01/, 2019.
- [29] J. N. Reddy, 2017, *Energy principles and variational methods in applied mechanics*, John Wiley & Sons,
- [30] X.-F. Li, A unified approach for analyzing static and dynamic behaviors of functionally graded Timoshenko and Euler-Bernoulli beams, *Journal of Sound and Vibration*, Vol. 318, pp. 1210-1229, 12/01, 2008.